

---

# Reward-Respecting Subtasks for Model-Based Reinforcement Learning

---

Richard S. Sutton<sup>1,2,3</sup> Marlos C. Machado<sup>1,2,3</sup> G. Zacharias Holland<sup>1</sup>  
 David Szepesvari<sup>1</sup> Finbarr Timbers<sup>1</sup> Brian Tanner<sup>1</sup> Adam White<sup>1,2,3</sup>

## Abstract

To achieve the ambitious goals of artificial intelligence, reinforcement learning must include planning with a model of the world that is abstract in state and time. Deep learning has made progress in state abstraction, but, although the theory of time abstraction has been extensively developed based on the options framework, in practice options have rarely been used in planning. One reason for this is that the space of possible options is immense and the methods previously proposed for option discovery do not take into account how the option models will be used in planning. Options are typically discovered by posing subsidiary tasks such as reaching a bottleneck state, or maximizing a sensory signal other than the reward. Each subtask is solved to produce an option, and then a model of the option is learned and made available to the planning process. The subtasks proposed in most previous work ignore the reward on the original problem, whereas we propose subtasks that use the original reward plus a bonus based on a feature of the state at the time the option stops. We show that options and option models obtained from such reward-respecting subtasks are much more likely to be useful in planning and can be learned online and off-policy using existing learning algorithms. Reward respecting subtasks strongly constrain the space of options and thereby also provide a partial solution to the problem of option discovery. Finally, we show how the algorithms for learning values, policies, options, and models can be unified using general value functions.

into improvements in its policy and, commonly, in its approximate value function. The conversion process, generically referred to as *planning*, is typically computationally expensive and may be distributed over many time steps (or even performed offline). MBRL is well-suited to environments whose transition dynamics are relatively simple but whose policy or value function are complex (such as in Chess and Go). More generally, MBRL may enable dramatically faster adaptation whenever the agent is long-lived, the environment is non-stationary, and much of the environment’s transition dynamics are stable (as approximately modeled by the agent). These are the properties that we see as applying to animals (including people) operating in the real world.

For planning to be tractable on large problems, an AI agent’s model must be abstract in state and time. Abstraction in state is important because the original states of the world may be too numerous to deal with individually, or may not be observable by the agent. In these cases, how the state should be constructed from observations is an important problem on which much work has been done with deep learning, in particular with LSTMs (Hochreiter & Schmidhuber, 1997) and in other ways (e.g., Lecun, Bottou, Bengio, & Haffner, 1998; Mnih et al., 2015). We do not address state abstraction in this paper other than by allowing the agent’s state representation to be a non-Markov feature vector.

This paper concerns how we should create and work with environment models that are abstract in *time*. The most common way of formulating temporally-extended and temporally-variable ways of behaving in a reinforcement learning agent is as *options* (Sutton, Precup, & Singh, 1999), each of which comprises a way of behaving (a policy) and a way of stopping. The appeal of options is that they are in some ways interchangeable with actions. Just as we can learn models of action’s consequences and plan with those models, so we can learn and plan with models of options’ effects. There remains the critical question of where the options come from. A common approach to option discovery is to pose subsidiary tasks such as reaching a bottleneck state or maximizing a sensory signal. Given a subtask, the agent can then develop temporally abstract structure for its cognition by following a standard progression, in which the subtask is solved to produce an option, the op-

In model-based reinforcement learning (MBRL), a reinforcement learning agent learns a model of the transition dynamics of its environment and then converts that model

<sup>1</sup>DeepMind. <sup>2</sup>University of Alberta, Edmonton, AB, Canada. <sup>3</sup>Alberta Machine Intelligence Institute (Amii). Correspondence to: Marlos C. Machado <marlosm@deepmind.com>.

tion’s consequences are learned to produce a model, and the model is used in planning. We refer to this progression (SubTask, Option, Model, Planning) as the STOMP progression for the development of temporally-abstract cognitive structure. All the steps of the STOMP progression were described in the original paper on options (Sutton et al., 1999), and it has been used in several previous works (e.g., Silver & Ciosek, 2012; Singh, Barto, & Chentanez, 2004; Sorg & Singh, 2010).

The conceptual innovation of the current work is to introduce the notion of a *reward-respecting* subtask, that is, of a subtask that optimizes the rewards of the original task until terminating in a state that is sometimes of high value. Reward-respecting subtasks contrast with commonly used subtasks, such as shortest path to bottleneck states (e.g., McGovern & Barto, 2001; Simsek & Barto, 2004; Simsek, Wolfe, & Barto, 2005), pixel maximization (Jaderberg et al., 2017), and diffusion maximization (c.f. Machado, Barreto, & Precup, 2021), which explicitly maximize the cumulative sum of a signal other than the reward of the original task.

For example, consider the two-room gridworld shown inset in Figure 1, with a start state in one room, a terminal goal state in the other, and a hallway state in-between. The usual four actions move the agent one cell up, down, right, or left unless blocked by a wall. A reward of +1 is received on reaching the goal state, which ends the episode. Transitions ending in the gray region between the start and hallway states produce a reward of  $-1$  per step, while all other transitions produce a reward of zero. The discount factor is  $\gamma = 0.99$ , so the optimal path from start to goal, traveling the roundabout path that avoids the field of negative reward, yields a return of  $0.99^{18} \approx 0.83$ . The hallway state is a bottleneck and thus a natural terminating subgoal for a subtask on this problem (as in Solway et al., 2014). With a reward-respecting subtask, the agent would learn a way to the hallway that maximizes the reward along the way; in this gridworld it finds the option that goes down from the start state and *around* the field of negative rewards. In contrast, solving the version of this subtask that does not take the reward into consideration would be to learn the shortest path from start to hallway, passing *through* the field of negative rewards.

Which of these two options are more useful when their models are learned and used in planning? Assuming the optimal options for both subtasks, and that all the models of the options and actions are known exactly, we can contrast the progress of planning by value iteration (as detailed later in this paper) with the primitive actions only, and with the primitive actions augmented by the models of the two options. The results, shown in Figure 1, are much as you would expect. Planning using the shortest-path option is less efficient than when using primitive actions only; likely

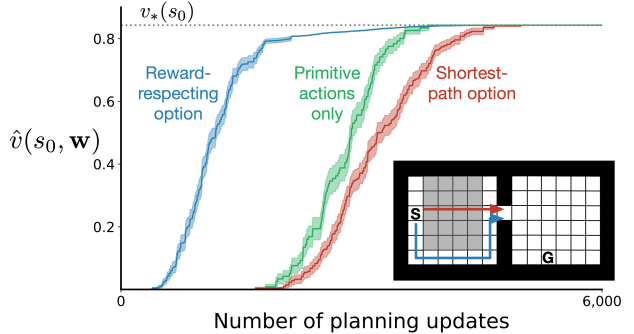


Figure 1. A gridworld example contrasting the progress of planning with reward-respecting options, with shortest-path options, and without options. Planning with reward respecting options is much faster in terms of number of states updated. Each line is averaged over 100 runs and the shading represents the standard error. See text for details.

because the option being considered is *not* part of the final solution. Importantly, planning with the model of the option based on the reward-respecting subtask is most efficient. In all cases the optimal policy is found and the value of the start state is eventually correctly estimated as  $\approx 0.83$ .

## 1. Reward-respecting subtasks

In this section we define the agent–environment interaction, the primary task, GVF subtasks, reward-respecting subtasks, and the reward-respecting subtask used to produce Figure 1. This is the first step in the STOMP progression for developing temporally-abstract cognitive structure.

We consider an agent interacting with an environment in a sequence of episodes, each beginning in environment state  $S_0 \in \mathcal{S}$  and ending in the terminal state  $S_L = \perp$  at time step  $L \in \mathbb{N}$ . At time steps  $t < L$ , the agent selects an action  $A_t \in \mathcal{A}$ , and in response the environment emits a reward  $R_{t+1} \in \mathcal{R} \subset \mathbb{R}$  and transitions to a next state  $S_{t+1} \in \mathcal{S} + \perp$  with probability  $p(s', r | s, a) \doteq \Pr\{S_{t+1} = s', R_{t+1} = r \mid S_t = s, A_t = a\}$ , where  $\mathcal{A}$ ,  $\mathcal{S}$ , and  $\mathcal{R}$  are all finite sets. Capitalized letters ( $S_t$ ,  $A_t$ ,  $R_t$ , and  $L$ ) denote random variables that differ from episode to episode; technically these should be indexed by an episode number, but we suppress that in our notation. The agent’s primary task is to find a policy  $\pi : \mathcal{S} \times \mathcal{A} \rightarrow [0, 1]$  that maximizes the expected discounted sum of rewards on an episode,  $\mathbb{E}[R_1 + \gamma R_2 + \dots + \gamma^{L-1} R_L]$ , where  $\gamma \in [0, 1)$  is the discount rate, a parameter of the problem.

Solution methods for the primary task often involve approximating the value function  $v_\pi : \mathcal{S} \rightarrow \mathbb{R}$  for the agent’s current policy  $\pi$ , defined by

$$v_\pi(s) \doteq \mathbb{E}_\pi \left[ \sum_{j=1}^L \gamma^{j-1} R_j \mid S_0 = s \right], \forall s \in \mathcal{S}, \quad (1)$$

where the expectation is conditional on the actions being selected according to  $\pi$ . In the current work we are particularly concerned with linear approximations to  $v_\pi$ . In this case, each state is converted to a feature vector by a function  $\mathbf{x} : \mathcal{S} \rightarrow \mathbb{R}^d$  (with  $\mathbf{x}(\perp) \doteq \vec{0}$ ), which might be all the layers of a neural network except for the last, or might be provided by a domain expert, and then  $v_\pi(s)$  is approximated as linear in  $\mathbf{x}(s)$  and a modifiable weight vector  $\mathbf{w} \in \mathbb{R}^d$ :

$$v_\pi(s) \approx \hat{v}(\mathbf{x}(s), \mathbf{w}) \doteq \mathbf{w}^\top \mathbf{x}(s) \doteq \sum_{i=1}^d w_i x_i(s), \quad (2)$$

for all  $s \in \mathcal{S}$ , where  $w_i$  and  $x_i(s)$  are individual components of  $\mathbf{w}$  and  $\mathbf{x}(s)$ , respectively.

We now generalize the primary task to include a full range of tasks for the episodic setting, based on the framework of general value functions (GVFs) introduced for the Horde architecture (Sutton et al., 2011). Instead of maximizing the sum of rewards  $R_t$ , we maximize the sum of a cumulant  $C_t \doteq c(S_t)$  for some function  $c : \mathcal{S} \rightarrow \mathbb{R}$ . Instead of the accumulation stopping only at the terminal state, it stops at every state with probability  $\beta(S_t)$  for some function  $\beta : \mathcal{S} \rightarrow [0, 1]$  (with  $\beta(\perp) \doteq 1$ ). Upon stopping, there is an additional contribution to the accumulation, a final *stopping value*  $z(S_t)$  for some function  $z : \mathcal{S} \rightarrow \mathbb{R}$  (with  $z(\perp) \doteq 0$ ). The functions  $c, z$  define the task, and the policy and stopping function,  $\pi, \beta$ , which together constitute an *option*,<sup>1</sup> define an attempted solution to the task. If option  $\langle \pi, \beta \rangle$  were initiated in state  $S_t$ , then  $A_t$  and subsequent actions would be selected according to  $\pi$  until the option ended, or *stopped*, according to  $\beta$  at step  $K$ . Given a GVF task  $c, z$ , the objective is to find an option that maximizes  $\mathbb{E}[C_1 + \gamma C_2 + \dots + \gamma^{K-1} C_K + \gamma^{K-1} z(S_K)]$  for whatever state  $S_0$  the option is started in. That is, the objective is to maximize the general value function:

$$v_{\pi, \beta}^{c, z}(s) \doteq \mathbb{E}_{\pi, \beta} \left[ \sum_{j=1}^K \gamma^{j-1} c(S_j) + \gamma^{K-1} z(S_K) \mid S_0 = s \right], \quad (3)$$

where the expectation is conditional on the actions being determined by  $\pi$  and the stopping time  $K$  being determined by  $\beta$ . Note that “stopping” is not termination, as it does not affect the actual flow of events in the trajectory. The primary task is a special case of a GVF task in which  $C_t \doteq R_t$  and  $Z_t \doteq -\infty, \forall t < L$ . Shortest path subtasks are defined by  $C_t \doteq -1$  and  $z(s) \doteq 0$  at subgoal states and  $z(s) \doteq -\infty$  otherwise. GVF tasks includes all the common subtasks in the literature including (if we allow the state to formally include agent-internal variables) all those based on curiosity and other intrinsic motivations (e.g., Baranes & Oudeyer, 2013; Eysenbach et al., 2019).

*Reward-respecting subtasks* are GVF tasks whose cumulant is identical with the reward,  $C_t = R_t$ , and whose stopping

values take into account the estimated value of the state stopped in. The stopping values cannot be equal to the estimated values, as then the subtask would approximate the primary task (exactly, in the tabular case) and solving it would add nothing new.

In this paper we consider *reward-respecting subtasks of feature attainment*, in which the objective is to maximize an individual feature of the state representation at stopping time while being mindful of the rewards received along the way. There will be many such subtasks, and we will use the superscript position to indicate the task number. For now we assume that we can have at most one task per feature, so the feature index  $i$  can serve double duty as a task number. The subtask for maximizing feature  $i$  has stopping-value function  $z^i$ :

$$z^i(s) \doteq \hat{v}(\mathbf{x}(s), \mathbf{w}) + x_i(s)(\bar{w}^i - w_i), \quad (4)$$

where  $\mathbf{w}$  and its  $i$ th component,  $w_i$ , are the weights for approximating the primary task, and  $\bar{w}^i$  is a *bonus weight* for subtask  $i$ , provided as part of defining the subtask. Note that under the linear form for  $\hat{v}$  (2),  $z^i$  does not depend on  $w_i$ . The quantity  $\bar{w}^i x_i$  is called the *stopping bonus*. Generally, it is only useful to construct subtasks for attaining a feature  $i$  if its contribution to value on the primary task,  $w_i$ , is sometimes high and sometimes low. If  $w_i$  never varied, then its static value could be fully taken into account without planning. If  $w_i$  does vary, then its bonus weight should be set to one of its higher values so that an option can be learned in preparation for the occasional times at which  $w_i$  is high.

Finally, the reward-respecting subtask used in producing Figure 1 was for the tabular feature for the hallway state, with bonus weight  $\bar{w}^h = 1$ , where  $h$  denotes the index of the feature for the hallway state. The shortest-path subtask used  $C_t = -1$  and stopped upon reaching the hallway or terminal goal states.

## 2. Option learning for feature attainment

In this section we specify the off-policy learning algorithms we use to approximate the optimal value functions and optimal options. This is the second step in the STOMP progression for developing temporally-abstract cognitive structure.

Define the *optimal value function*  $v_*^i : \mathcal{S} \rightarrow \mathbb{R}$  for the reward-respecting subtask for attaining the  $i$ th feature by (3) with  $C_t \doteq R_t$ ,  $z \doteq z^i$ , and the  $\pi$  and  $\beta$  that maximize the value. Define the *optimal option* as that pair  $\langle \pi, \beta \rangle$ . We will describe these algorithms in a somewhat unusual way that lets us cover all the cases very compactly and uniformly, including the model learning in the next section. First we define a general TD (Temporal Difference) error function

<sup>1</sup>Options sometimes also include a condition on the states in which the option can be initiated, but we do not use that here.

$\delta : \mathbb{R}^4 \times [0, 1] \rightarrow \mathbb{R}$ :

$$\delta(c, z, v, v', \beta) \doteq c + \beta z + \gamma(1-\beta)v' - v. \quad (5)$$

We use various TD errors to specify our learning algorithms, together with a general update procedure for learning with traces, which we call *UpdateWeights&Traces* (UWT):

**Procedure UWT**( $\mathbf{w}, \mathbf{e}, \nabla, \alpha\delta, \rho, \gamma\lambda(1-\beta)$ ):

$$\begin{aligned} \mathbf{e} &\leftarrow \rho(\mathbf{e} + \nabla) \\ \mathbf{w} &\leftarrow \mathbf{w} + \alpha\delta\mathbf{e} \\ \mathbf{e} &\leftarrow \gamma\lambda(1-\beta)\mathbf{e} \end{aligned}$$

The first two arguments to UWT are a weight vector and an eligibility-trace vector. These arguments are both inputs and outputs; the same pair are expected to be provided together on every time step. The weight vector is the ultimate result of learning. The eligibility trace is a short-term memory that helps with credit assignment. The third argument is usually a gradient vector with respect to the weight vector. The fourth and sixth arguments to UWT are scalars—the names of the formal arguments are just suggestive of their use. Finally, the fifth argument is a scalar importance-sampling ratio used in off-policy learning (for on-policy learning it should be one).

Here is how these tools would be used to implement on-policy linear TD( $\lambda$ ) (Sutton, 1988) on the primary task. First we would zero-initialize  $\mathbf{w}$  and corresponding eligibility-trace vector  $\mathbf{e} \in \mathbb{R}^d$ . Then we would have the agent behave according to some policy  $\pi$  and, on each time step in which  $S_t$  is nonterminal, we would do:

$$\delta \leftarrow \delta(R_{t+1}, 0, \hat{v}(\mathbf{x}_t, \mathbf{w}), \hat{v}(\mathbf{x}_{t+1}, \mathbf{w}), 0), \text{ and} \quad (6)$$

$$\text{UWT}(\mathbf{w}, \mathbf{e}, \nabla_{\mathbf{w}}\hat{v}(\mathbf{x}_t, \mathbf{w}), \alpha\delta, 1, \gamma\lambda), \quad (7)$$

where  $\alpha$  and  $\lambda$  are step-size and bootstrapping parameters. Note that in the linear case,  $\nabla\hat{v}(\mathbf{x}_t, \mathbf{w})$  in (7) is just  $\mathbf{x}_t$ . Now suppose the policy  $\pi$  is parameterized by  $\boldsymbol{\theta} \in \mathbb{R}^d$  and we wanted to learn it as well, in an actor-critic algorithm (Sutton, 1984). This would be achieved by invoking UWT one more time on each step, immediately after (7):

$$\text{UWT}(\boldsymbol{\theta}, \mathbf{e}', \nabla_{\boldsymbol{\theta}} \ln \pi(A_t|S_t, \boldsymbol{\theta}), \alpha'\delta, 1, \gamma\lambda'), \quad (8)$$

where  $\mathbf{e}' \in \mathbb{R}^d$  is another zero-initialized eligibility-trace vector, and  $\alpha'$  and  $\lambda'$  are step-size and bootstrapping parameters for the actor.

Now we show how to use these tools to learn the value functions and options for the subtasks, off-policy. Let  $\mathcal{F} \subset \{0, \dots, d\}$  be the set of features for which we have subtasks. Each subtask will have a weight vector  $\mathbf{w}^i \in \mathbb{R}^d$  such that  $\hat{v}(\mathbf{x}(s), \mathbf{w}^i) \doteq \mathbf{w}^{i\top} \mathbf{x}(s)$  approximates a GVF (2) where  $C_t = R_t$ ,  $z = z^i$  (4),  $\pi = \pi(\cdot|\cdot, \boldsymbol{\theta}^i)$ , where  $\boldsymbol{\theta}^i \in \mathbb{R}^d$  is another modifiable weight vector, and  $\beta = \beta^i$ , defined by

$$\beta^i(s) \doteq \begin{cases} 1, & \text{if } z^i(s) \geq \mathbf{w}^{i\top} \mathbf{x}(s); \\ 0, & \text{otherwise,} \end{cases} \quad (9)$$

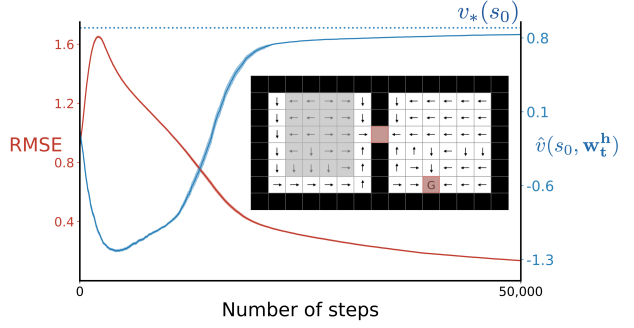


Figure 2. The off-policy learning algorithm applied to find the optimal option for the reward-respecting subtask for attaining the hallway feature. The data comes from a policy in which all four actions were selected with equal probability. Shown with arrows is a representation of the policy learned after 50,000 steps; the red cells are those in which the agent learned to stop. The option shown is from a single run of the system, whereas each line is averaged over 100 runs and the shading represents the standard error. The learned option avoids the negative-reward region on the way to the hallway state (gray region), while the policy mostly moves toward the goal in the second room. The plot shows the progress of learning. The blue line (right scale) shows the value of the start state for the learned option, and the red line (left scale) shows the RMSE between the learned and optimal value functions.

for all  $s \in \mathcal{S}$ , with  $\beta^i(\perp) \doteq 1$ . We will be learning off-policy, so we will need the importance sampling ratios

$$\rho_t^i \doteq \frac{\pi(A_t|S_t, \boldsymbol{\theta}^i)}{\mu(A_t|S_t)}, \quad (10)$$

where  $\mu : \mathcal{A} \times \mathcal{S} \rightarrow [0, 1]$  is the *behavior policy* (the policy actually used to select actions, as opposed to the policies being learned about). For each subtask  $i \in \mathcal{F}$ , in addition to  $\mathbf{w}^i$  and  $\boldsymbol{\theta}^i$  we will also have eligibility-trace vectors  $\mathbf{e}^i \in \mathbb{R}^d$  and  $\mathbf{e}'^i \in \mathbb{R}^d$ , all initialized to zero. Then, on each time step on which  $S_t$  is nonterminal, for each  $i \in \mathcal{F}$  we do:

$$\begin{aligned} \delta &\leftarrow \delta(R_{t+1}, z_{t+1}^i, \hat{v}(\mathbf{x}_t, \mathbf{w}^i), \hat{v}(\mathbf{x}_{t+1}, \mathbf{w}^i), \beta_{t+1}^i), \\ \text{UWT}(\mathbf{w}^i, \mathbf{e}^i, \nabla_{\mathbf{w}^i}\hat{v}(\mathbf{x}_t, \mathbf{w}^i), \alpha\delta, \rho_t^i, \gamma\lambda(1-\beta_{t+1}^i)), \text{ and} \\ \text{UWT}(\boldsymbol{\theta}^i, \mathbf{e}'^i, \nabla_{\boldsymbol{\theta}^i} \ln \pi(A_t|S_t, \boldsymbol{\theta}^i), \alpha'\delta, \rho_t^i, \gamma\lambda'(1-\beta_{t+1}^i)), \end{aligned}$$

where here we use the shorthands  $z_t^i \doteq z^i(S_t)$  and  $\beta_t^i \doteq \beta^i(S_t)$ . Under this algorithm, the learned approximate values  $\hat{v}(\mathbf{x}(s), \mathbf{w}^i) \doteq \mathbf{w}^{i\top} \mathbf{x}(s)$  come to approximate the *optimal subtask values*  $v_*^i(s) \doteq \max_{\pi, \beta} v_{\pi, \beta}^i(s)$ ,  $\forall s \in \mathcal{S}$  and  $i \in \mathcal{F}$ , and the options  $\langle \pi(\cdot|\cdot, \boldsymbol{\theta}^i), \beta^i \rangle$  come to approximate the corresponding optimal options. In the tabular case, the approximations become exact with sufficient exploration and if the step sizes are decreased appropriately.

Figure 2 shows such exact convergence for the hallway-feature attaining subtask. We used a behavior policy that selected all four actions with equal probability:  $\mu(a|s) \doteq 0.25, \forall s \in \mathcal{S}, a \in \mathcal{A}$ . The state-feature vectors were 1-hot, producing a tabular representation with  $d = 72$  for the 72

non-terminal grid cells. The policy was of the softmax form with linear preferences:

$$\pi(a|s, \theta) \doteq \frac{e^{\theta^\top \phi(s,a)}}{\sum_b e^{\theta^\top \phi(s,b)}}, \quad (11)$$

where the state-action feature vectors  $\phi(s, a) \in \mathbb{R}^{d'}$ ,  $\forall s \in \mathcal{S}$ ,  $a \in \mathcal{A}$  were again 1-hot or tabular ( $d' = 288$ ). We ran for 50,000 steps and averaged the results over 100 runs.

Figure 2 depicts the root mean squared error, throughout time, between the estimated subtask value,  $\hat{v}(S_t, \mathbf{w}_t^h)$ , for the subtask for attaining the  $h$ th feature, corresponding to the hallway state, and the optimal subtask value,  $v_*^h(S_t)$ . The curve shows the actor-critic algorithm is able to effectively learn the correct option policy. Notice that the option terminates either at the bottleneck state or the goal state, as shown in red. Reward-respecting options trade off rewards, the value of the state, and the stopping bonus. In the right room, close to the bottleneck state it is more beneficial to go to the bottleneck state because the stopping bonus plus the value of that state is greater than the value of directly going to the goal state. In states closer to the goal state, it is better to directly go to the goal state rather than to go back to the hallway.

### 3. Model learning

In this section we describe the third step in the STOMP progression: learning a model of the environment’s action and option transitions. Recall that an option is a pair,  $o \doteq \langle \pi_o, \beta_o \rangle$ , consisting of a policy and a stopping function. Actions are a special case of options in which the policy  $\pi_o$  always selects the action and the stopping function always stops,  $\beta_o(s) = 1, \forall s \in \mathcal{S}$ . Let  $\mathcal{O}(s)$  denote the set of options (including actions) available in state  $s$ , and let  $\mathcal{O}$  denote the set of all options (unioning over all states). With a slight abuse of notation, we allow  $\mathcal{O}$  to also include the indices of state-features  $i \in \mathcal{F}$  for which the agent has learned an option; when that feature index appears in a position that is expecting an option (as in the next few equations) we mean the option corresponding to that feature.

The *idealized* model is expressed in terms of the underlying environment states  $s \in \mathcal{S}$  and exactly matches the true underlying dynamics. Like all models, it is comprised of a reward part and a state-transition part. The reward part is a function  $r : \mathcal{S} \times \mathcal{O} \rightarrow \mathbb{R}$  returning the expected cumulative discounted reward if the option were executed starting from the state:

$$r(s, o) \doteq \mathbb{E}_{\pi_o, \beta_o} \left[ \sum_{j=1}^K \gamma^{j-1} R_{t+j} \mid S_t = s \right], \quad (12)$$

for all  $o \in \mathcal{O}$  and  $s \in \mathcal{S}$ , and where the expectation is conditional on actions being selected by  $\pi_o$  and  $K$  being determined by  $\beta_o$ . The state-transition part of an idealized

model is a function  $p : \mathcal{S} \times \mathcal{S} \times \mathcal{O} \rightarrow [0, 1]$  returning, for each state  $s$  in which an option might be started, the probability of stopping in each state  $s'$ , discounted by the time until stopping:

$$p(s'|s, o) \doteq \sum_{k=1}^{\infty} \gamma^k \Pr\{K = k, S_{t+k} = s' \mid S_t = s\}, \quad (13)$$

for all  $o \in \mathcal{O}$  and  $s, s' \in \mathcal{S}$ , and where the probability is conditional on the actions from  $t$  being selected according to the policy of option  $o$  and  $K$  being determined by its stopping function. Note that we write the  $p$  function with a  $|$ , suggesting that it is a probability distribution, but for  $\gamma < 1$  it is not. This precise form is dictated by the requirement that option models and action models be interchangeable in planning methods such as value iteration (see next section).

Approximate models do not in general have access to environmental states, but instead must work with a representation of state constructed by the agent, which might be called the *agent state*. Unlike the environment state, the agent state is generally not a Markov summary of the past. In this paper we assume the agent state is a state-feature vector  $\mathbf{x} \in \mathbb{R}^d$  (in the tabular special case these would be 1-hot vectors and they would be Markov) which can be determined from the environment state by a known function  $\mathbf{x} : \mathcal{S} \rightarrow \mathbb{R}^d$ . The reward part of an approximate model of an option is a function  $\hat{r} : \mathbb{R}^d \times \mathcal{O} \rightarrow \mathbb{R}$  such that

$$\hat{r}(\mathbf{x}(s), o) \approx r(s, o), \quad \forall s \in \mathcal{S}, \quad (14)$$

weighted over some distribution of states such as the state distribution under the behavior policy. The state-transition part of an approximate model could take several forms. In an *expectation* model, the state-transition part is a function  $\hat{\mathbf{n}} : \mathbb{R}^d \times \mathcal{O} \rightarrow \mathbb{R}^d$  such that

$$\hat{\mathbf{n}}(\mathbf{x}(s), o) \approx \sum_{s' \in \mathcal{S}} p(s'|s, o) \mathbf{x}(s') \quad (15)$$

$$= \mathbb{E}_o[\gamma^K \mathbf{x}(S_{t+K}) \mid S_t = s], \quad (16)$$

for all  $s \in \mathcal{S}$  under some state weighting, perhaps given by the behavior policy, and where the expectation is conditional on the actions being selected according to  $o$ ’s policy and the stopping time  $K$  being determined by  $o$ ’s stopping function.

For the illustrative example in Figure 1, we learned models for the four options corresponding to the actions and the reward-respecting option for the hallway state. The approximate model was linear in the state-feature vector, meaning that

$$\hat{r}(\mathbf{x}, o) \doteq \mathbf{w}_r^o \top \mathbf{x}, \quad (17)$$

where each  $\mathbf{w}_r^o \in \mathbb{R}^d$  is a learned weight vector, and

$$\hat{\mathbf{n}}(\mathbf{x}, o) \doteq \mathbf{W}^o \mathbf{x}, \quad (18)$$

where each  $\mathbf{W}^o$  is a  $d \times d$  matrix, with rows  $\mathbf{w}_j^o$ . In this tabular problem ( $d = |\mathcal{S}| = 72$ ) the states were represented

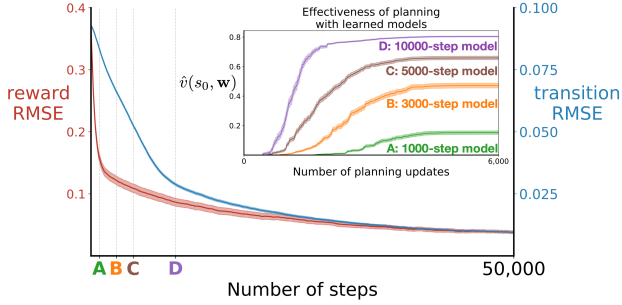


Figure 3. Transition and reward models are efficiently learned on-line. The red line (left scale) shows the root mean square error (RMSE) between the learned reward model for the option and the idealized reward model. The blue line (right scale) shows the RMSE between the learned transition model for the option and the idealized state-transition model. The state-transition model captures discounting and termination. The performance of planning for learned, approximate models with different levels of accuracy is depicted in the inset plot. In this environment, 17,000 steps of model learning is sufficient to achieve near-optimal planning performance. All lines were averaged over 100 runs and the shading represents the standard error. See appendix for other details.

by 1-hot feature vectors. To learn the weights, each weight vector (the  $\mathbf{w}_r^o$  and the  $\mathbf{w}_j^o$ , for  $o \in \mathcal{O}$ ,  $j = 1, \dots, d$ ) was paired with an eligibility trace vector,  $\mathbf{e}_r^o$  and the  $\mathbf{e}_j^o$ s. All these vectors were initialized to zero. The agent wandered all over the two rooms following the equi-probable random policy for many episodes. On each step ( $S_t, A_t, R_{t+1}, S_{t+1}$ ) for which  $S_t$  was non-terminal, for each  $o \in \mathcal{O}$ , we did:

$$\delta \leftarrow \delta(R_{t+1}, 0, \hat{r}(\mathbf{x}_t, o), \gamma \hat{r}(\mathbf{x}_{t+1}, o), \beta_{t+1}^o) \quad (19)$$

$$\text{UWT}(\mathbf{w}_r^o, \mathbf{e}_r^o, \nabla \hat{r}(\mathbf{x}_t, o), \alpha_r \delta, \rho_t^o, \gamma \lambda (1 - \beta_{t+1}^o)) \quad (20)$$

and, for each  $j = 1, \dots, d$ :

$$\delta \leftarrow \delta(0, \gamma x_{j,t+1}, \hat{n}_j(\mathbf{x}_t, o), \gamma \hat{n}_j(\mathbf{x}_{t+1}, o), \beta_{t+1}^o) \quad (21)$$

$$\text{UWT}(\mathbf{w}_j^o, \mathbf{e}_j^o, \nabla \hat{n}_j(\mathbf{x}_t, o), \alpha_p \delta, \rho_t^o, \gamma \lambda (1 - \beta_{t+1}^o)), \quad (22)$$

where  $x_{j,t+1}$  denotes the  $j$ th component of  $\mathbf{x}_{t+1}$ ,  $\hat{n}_j$  denotes the  $j$ th component of the vector returned by  $\hat{\mathbf{n}}$ , and  $\beta_t^i \doteq \beta^i(S_t)$ . This way of using TD( $\lambda$ ) algorithms to learn a temporally abstract model of the world was introduced by Sutton (1995; see also Sutton and Barto, 2018, Section 17.2) Note that for one-step options such as actions, the use of UWT is not necessary; the algorithm is correct as specified, but if desired it could be implemented more efficiently without eligibility traces.

The procedure described above allows us to efficiently learn both transition and reward models, as shown in Figure 3. We also evaluated the impact of planning with imperfect models, using the planning algorithm described in the next section. The results are shown in the inset plot. Planning leads to near-optimal performance using an imperfect model trained for 17,000 steps. Further training improves model

error but does not significantly improve planning in this environment.

It can be advantageous to learn a linear expectation model under function approximation. In the general case, the transition-part must be able to produce the entire distribution of resultant states. These *distribution* models are important theoretically and have been used effectively when the possible distributions can be assumed to be of a special form (e.g., Gaussian), as in the PILCO method (Deisenroth & Rasmussen, 2011). Generally, these are very large objects and would be hopelessly unwieldy for large  $d$ . Fortunately, if the value function is linear in the state features, then there is no loss of generality when using an expectation model in planning (Wan et al., 2019, Kudashkina, 2022).

#### 4. Planning with options and approximations

Our planning method approximates *value iteration*, the classical planning algorithm for finite MDPs, in its asynchronous form extended to options (Sutton, Precup, & Singh, 1999). In that tabular algorithm, the state-value estimates  $V(s), \forall s \in \mathcal{S}$ , are initialized arbitrarily and then updated one-by-one, in some sequence, by:

$$V(s) \leftarrow \max_{o \in \mathcal{O}(s)} [r(s, o) + \sum_{s'} p(s'|s, o) V(s')], \quad (23)$$

where  $r$  and  $p$  are the reward and state-transition parts of the idealized model of option  $o$ , as defined in the previous section, and  $\mathcal{O}(s)$  is the set of options considered in state  $s$ , which may include all or some of the primitive actions available. If  $\mathcal{O}(s)$  is exactly the primitive actions, then  $\hat{p}(s'|s, o)$  is exactly the state-transition probabilities, times  $\gamma$ , and the general form (23) reduces to classical value iteration.

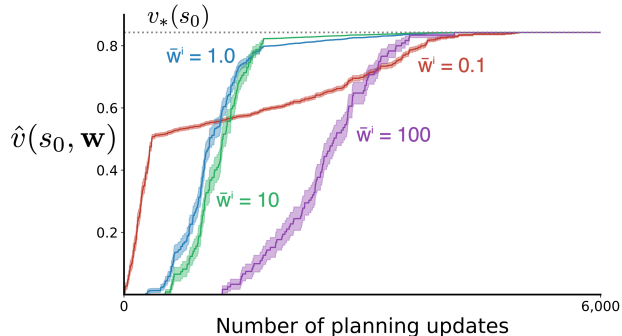
In our planning method, *approximate value iteration* (AVI), the estimated value function is maintained not as a table  $V(s)$ , but as a parameterized form  $\hat{v}(\mathbf{x}(s), \mathbf{w})$  with parameter  $\mathbf{w} \in \mathbb{R}^d$  with  $d \ll |\mathcal{S}|$ . Moreover, the planner will iterate over state-feature vectors  $\mathbf{x} \in \mathbb{R}^d$  instead of environmental states  $s \in \mathcal{S}$ . In this paper we use a linear form  $\hat{v}(\mathbf{x}, \mathbf{w}) \doteq \mathbf{w}^\top \mathbf{x}$ , which combines favorably with expectation models, but in general any differentiable parameterized form could be used. The parameter vector  $\mathbf{w}$  is initialized arbitrarily and then updated, for each state-feature vector  $\mathbf{x}$ , in some sequence of state-feature vectors, by

$$\mathbf{w} \leftarrow \mathbf{w} + \alpha \left[ \max_{o \in \mathcal{O}(\mathbf{x})} b(\mathbf{x}, o, \mathbf{w}) - \hat{v}(\mathbf{x}, \mathbf{w}) \right] \nabla_{\mathbf{w}} \hat{v}(\mathbf{x}, \mathbf{w}), \quad (24)$$

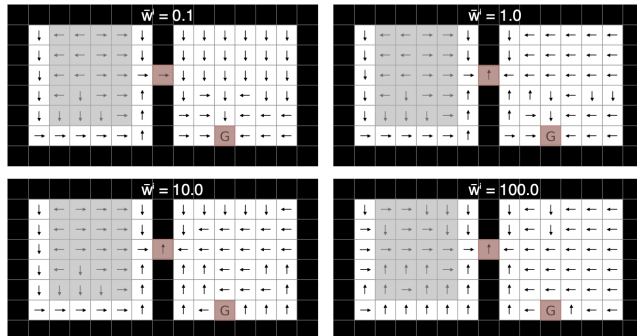
where  $\alpha > 0$  is a step-size parameter, and

$$b(\mathbf{x}, o, \mathbf{w}) \doteq \hat{r}(\mathbf{x}, o) + \hat{v}(\hat{\mathbf{n}}(\mathbf{x}, o), \mathbf{w}). \quad (25)$$

The quantity  $b(\mathbf{x}, o, \mathbf{w})$  is the *backed-up value* of the state represented by  $\mathbf{x}$ , when projected ahead by the model of



(a) Impact in planning induced by the reward-respecting options learned with different values of  $\bar{w}^i$  from (4). Each line is averaged over 100 runs and the shading represents the standard error.



(b) Reward-respecting options learned with different values of  $\bar{w}^i$ . The problem of option discovery can be summarized as the problem of defining  $z^i$ ; even different values of  $\bar{w}^i$  lead to different options.

Figure 4. Impact of different values of  $\bar{w}^i$  on the options learned and the induced planning performance. See Section 5 for details.

option  $o$ , using the approximate value function given by the weights  $\mathbf{w}$ . Using the backed-up value in (24) takes the place of the full sum in (23). This can only be done without introducing any additional approximation error if the value function involved is linear in the state-feature vector  $\mathbf{x}$  (Wan et al., 2019).

To obtain the results in Figure 1, we sampled states  $s$  randomly from the state set  $\mathcal{S}$ , computed their feature vectors  $\mathbf{x}(s)$ , and then applied (24) using (25). The weight vector  $\mathbf{w}$  was initialized to zero. The models of the actions and options were learned until near convergence as described in the preceding section.

The primary definition of a useful option is one that takes the maximum in (23) or (24) at some state and thus makes a difference in planning. We assume here that the model of the option has been learned and is stable, but the approximate value function has not been fully learned and is not stable (as otherwise no further planning would be necessary). These assumptions are noteworthy and deserve examination. Certainly there are cases where they are appropriate. In Chess, the model of the game’s dynamics is known completely, and could have been learned, but the value of almost all states can only be approximated, and the planning problem is so large that it is never completely solved and the state values are never all known exactly.

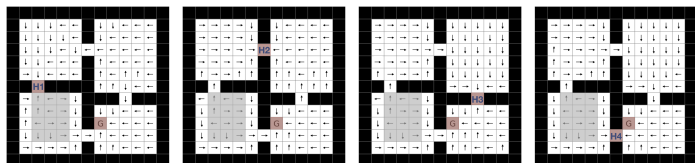
So, to make the backed-up values large, we certainly seek options for which  $r(s, o)$ , the cumulative reward during the option, is large. This is the main point about reward-respecting options. We also want the second term of the backed-up value to be large, which is achieved if the option terminates in states of high approximate value. That is, we seek options that produce high rewards and that drive the environment to states that, occasionally, have high value.

## 5. Stopping bonuses matter

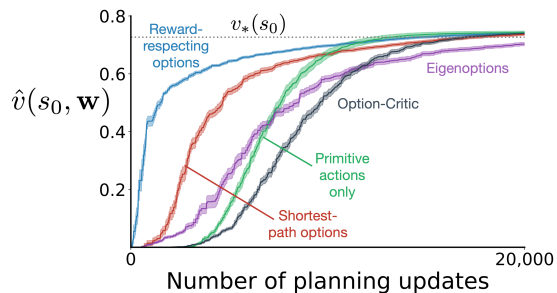
The definition of subtasks presented in Section 2 constrains the search space for option discovery. The magnitude of the bonus weight defines how much the agent wants to take the rewards observed along the way into consideration when compared to the agent’s estimated value of that state. Reward-respecting subtasks are a particular type of subtask defined by a cumulant and the value of the stopping state. Because the subtask’s cumulant is the reward, the value of the stopping state contains the only parameter of the subtask: the bonus weight,  $\bar{w}^i$ . So far, we only considered the case where  $\bar{w}^i = 1$ . We now evaluate the impact of different values of  $\bar{w}^i$  and show how different values allow us to approximate shortest-path options.

Figure 4 depicts the impact of different values of  $\bar{w}^i$  in the two-room gridworld. We report the progress of planning for different values of  $\bar{w}^i$ , having run all steps of the STOMP progression in order to generate the results. We also depict the options learned for different values of  $\bar{w}^i$  to illustrate how the options’ policies are impacted. The progress of option and model learning is unaffected by  $\bar{w}^i$ .

As expected, small values of  $\bar{w}^i$  make attaining feature  $i$  less important. In particular, when  $\bar{w}^i = 0.1$ , the agent avoids the region of negative rewards, but is much more interested in the goal state, as seen in the right room. Large values of  $\bar{w}^i$ , such as  $\bar{w}^i = 100$ , makes attaining feature  $i$  much more attractive, such that the reward-respecting option becomes the shortest-path option. Different values of  $\bar{w}^i$  also impact the degree to which the agent is willing to experience negative rewards in order to complete the subtask quicker (c.f.  $\bar{w}^i = 10$  vs.  $\bar{w}^i = 100$ ). Naturally, different options could make planning more or less effective.



(a) Reward-respecting options learned in a stochastic gridworld. Four options are learned as solutions to four subtasks seeking to attain the four hallway states (labeled H1-H4). Stochastic transitions make states close to the negative reward region (shaded gray) less desirable due to the natural uncertainty over their return.



(b) Progress of planning with different types of options in the four-rooms gridworld. Each line is averaged over 30 runs and the shading represents the standard error.

Figure 5. Illustration of the STOMP progression in a four-rooms problem. We include two baselines: the option-critic (Bacon et al., 2017) and eigenoptions (Machado et al., 2017, 2018). The option-critic parameterizes options’ policies and uses option-value functions and the policy gradient theorem to learn options that maximize the return. Eigenoptions are options designed for temporally-extended exploration that do not take rewards into consideration.

## 6. Multiple options and stochasticity

In this section we present results for a larger STOMP progression with multiple subtasks in a stochastic environment, and we compare reward-respecting options to other choices. Specifically, we used the four-room episodic gridworld depicted in Figure 5a, with a start state in one room, and a terminal goal state in another. As in the two-room gridworld, a reward of +1 is received on reaching the goal, which ends the episode, and passing through the gray region produces a reward of  $-1$  per step, while all other transitions produce a reward of zero. The discount factor is  $\gamma = 0.99$ . There are four actions, available in all nonterminal states: up, down, left, and right. Importantly, each action causes the agent to *stochastically* move in the corresponding direction with probability  $2/3$  and in one of the other three directions with probability  $1/9$ .

We defined four subtasks, each subtask directed toward reaching one of the four hallways states. The hallways are labeled in Figure 5a as H1-H4. Notice that reward-respecting options take into consideration the fact that the environment’s stochasticity is not under the agent’s control. For the most part, the options take the shortest path to the hallway or the goal state, but the uncontrolled stochasticity and the negative reward region causes some options to prefer a longer (and safer) path. For example, when in the South-West room, options sometimes take the roundabout way to reach H3 and H4.

Here, besides the shortest-path option, we consider *eigenoptions* (Machado et al., 2017; 2018) and the *option-critic* (Bacon, Harb, & Precup, 2017) as alternative option construction methods. The option-critic generates reward-respecting options that were not used for planning, and eigenoptions are options designed for model-free exploration, not planning, and which do not take the rewards into consideration. As aforementioned, in this paper we introduce general formulation of the option discovery problem (3). We can illustrate

that with eigenoptions, which can be seen as maximizing (3), but with  $C_t \doteq 0$  and  $z(S_K)$  being the value assigned by the eigenvector of the graph Laplacian to state  $S_K$ .

The results in Figure 5b show that reward-respecting options are more appropriate than alternative subtask formulations when these options are to be used in the STOMP progression. Moreover, considering multiple options in the STOMP progression does not impact performance. The stochastic nature of the environment also does not impact the applicability of the approach presented. The results for option and model learning, which are similar to those reported in previous sections, can be found in the Appendix.

## 7. Conclusions, limitations, and future work

In this paper, we introduced reward-respecting subtasks and showed how they lead to more efficient planning because they are more likely to be part of the agent’s final plan. We did so through the language of general value functions (GVFs), which allowed us to introduce a general procedure that unifies option learning, value learning, and model learning. Our formulation can also be seen as a formalization of the option discovery problem that unifies option discovery methods. We also introduced reward-respecting subtasks of feature attainment. This simple choice reduces the option discovery problem to one of deciding what features to maximize.

We have focused on presenting the problem formulation and each step of the STOMP progression in a general way in order to be amenable to different forms of function approximation. We considered only time abstraction, not state abstraction, but it is natural to ask how our approach would perform with different forms of function approximation. An interesting related question is how feature attainment interacts with representation learning techniques that automatically construct state abstractions.



## Acknowledgements

The authors would like to thank Francesco Visin for his feedback on an earlier draft; and Joseph Modayil, Martha White, and Michael Bowling for useful discussions. Richard S. Sutton, Marlos C. Machado and Adam White are supported by a Canada CIFAR AI Chair.

## References

- Bacon, P.-L., Harb, J., & Precup, D. (2017). The Option-Critic Architecture. In *Proceedings of the National Conference on Artificial Intelligence (AAAI)*.
- Baranes, A., & Oudeyer, P.-Y.. Active Learning of Inverse Models with Intrinsically Motivated Goal Exploration in Robots. *Robotics and Autonomous Systems*, 61(1): 49–73, 2013.
- Deisenroth, M. P., & Rasmussen, C. E. (2011). PILCO: A Model-Based and Data-Efficient Approach to Policy Search. In *Proceedings of the International Conference on Machine Learning (ICML)*.
- Eysenbach, B., Gupta, A., Ibarz, J., & Levine, S. (2019). Diversity is All You Need: Learning Skills without a Reward Function. In *Proceedings of the International Conference on Learning Representations (ICLR)*.
- Hochreiter, S., & Schmidhuber, J. (1997). Long Short-Term Memory. *Neural Computation*, 9(8), 1735–1780.
- Jaderberg, M., Mnih, V., Czarnecki, W. M., Schaul, T., Leibo, J. Z., Silver, D., & Kavukcuoglu, K. (2017). Reinforcement Learning with Unsupervised Auxiliary Tasks. In *Proceedings of the International Conference on Learning Representations (ICLR)*.
- Kudashkina, K. (2022). *Model-based Reinforcement Learning Methods for Developing Intelligent Assistants* (PhD dissertation). Department of Engineering, University of Guelph.
- Lecun, Y., Bottou, L., Bengio, Y., & Haffner, P. (1998). Gradient-based Learning Applied to Document Recognition. *Proceedings of the IEEE*, 86(11), 2278–2324.
- Machado, M. C., Barreto, A., & Precup, D. (2021). Temporal Abstraction in Reinforcement Learning with the Successor Representation. *ArXiv, abs/2110.05740*.
- Machado, M. C., Bellemare, M. G., & Bowling, M. H. (2017). A Laplacian Framework for Option Discovery in Reinforcement Learning. In *Proceedings of the International Conference on Machine Learning (ICML)*.
- Machado, M. C., Rosenbaum, C., Guo, X., Liu, M., Tesauro, G., & Campbell, M. (2018). Eigenoption Discovery through the Deep Successor Representation. In *Proceedings of the International Conference on Learning Representations (ICLR)*.
- McGovern, A., & Barto, A. G. (2001). Automatic Discovery of Subgoals in Reinforcement Learning using Diverse Density. In *Proceedings of the International Conference on Machine Learning (ICML)*.
- Mnih, V., Kavukcuoglu, K., Silver, D., Rusu, A. A., Veness, J., Bellemare, M. G., . . . Hassabis, D. (2015). Human-level Control through Deep Reinforcement Learning. *Nature*, 518, 529–533.
- Silver, D., & Ciosek, K. (2012). Compositional Planning Using Optimal Option Models. In *Proceedings of the International Conference on Machine Learning (ICML)*.
- Simsek, O., & Barto, A. G. (2004). Using Relative Novelty to Identify Useful Temporal Abstractions in Reinforcement Learning. In *Proceedings of the International Conference on Machine Learning (ICML)*.
- Simsek, O., Wolfe, A. P., & Barto, A. G. (2005). Identifying Useful Subgoals in Reinforcement Learning by Local Graph Partitioning. In *Proceedings of the International Conference on Machine Learning (ICML)*.
- Singh, S. P., Barto, A. G., & Chentanez, N. (2004). Intrinsically Motivated Reinforcement Learning. In *Advances in Neural Information Processing Systems (NeurIPS)*.
- Solway, A., Diuk, C., Cordova, N., Yee, D., Barto, A. G., Niv, Y., & Botvinick, M. (2014). Optimal Behavioral Hierarchy. *PLoS Computational Biology*, 10(8).
- Sorg, J., & Singh, S. P. (2010). Linear Options. In *Proceedings of the International Conference on Autonomous Agents and Multiagent Systems (AAMAS)*.
- Sutton, R. S. (1984). *Temporal Credit Assignment in Reinforcement Learning* (PhD dissertation). Department of Computer Science, University of Massachusetts, Amherst.
- Sutton, R. S. (1988). Learning to Predict by the Methods of Temporal Differences. *Machine Learning*, 3: 9–44.
- Sutton, R. S. (1995). TD Models: Modeling the World at a Mixture of Time Scales. In *Proceedings of the International Conference on Machine Learning (ICML)*.
- Sutton, R. S., & Barto, A. (2018). *Reinforcement Learning: An Introduction* (2nd ed.). MIT Press.
- Sutton, R. S., Modayil, J., Delp, M., Degris, T., Pilarski, P. M., White, A., & Precup, D. (2011). Horde: A Scalable Real-Time Architecture for Learning Knowledge from Unsupervised Sensorimotor Interaction. In *Proceedings of the International Conference on Autonomous Agents and Multiagent Systems (AAMAS)*.
- Sutton, R. S., Precup, D., & Singh, S. (1999). Between MDPs and semi-MDPs: A Framework for Temporal Abstraction in Reinforcement Learning. *Artificial Intelligence*, 112(1–2), 181–211.
- Wan, Y., Zaheer, M., White, A., White, M., & Sutton, R. S. (2019). Planning with Expectation Models. In *Proceedings of the International Joint Conference on Artificial Intelligence (IJCAI)*.

---

# Supplemental Material

## Reward-Respecting Subtasks for Model-Based Reinforcement Learning

---

### Organization of the Supplemental Material

- A. Details about empirical evaluation in the tabular case
  - A.1. Environment dynamics
  - A.2. Subtask specification
  - A.3. Option learning for feature attainment
  - A.4. Model learning
  - A.5. Planning
- B. Multiple options and stochasticity
  - B.1. Option learning for feature attainment
  - B.2. Model learning

### A. Details about empirical evaluation in the tabular case

In the main paper, when presenting empirical results, for better readability, we did not provide enough details to reproduce the reported results, such as the parameters used. We do so here.

#### A.1. Environment dynamics

In both the two-room and four-room gridworlds we use a tabular representation (i.e., one-hot encoding) and four primitive actions are available to the agent: `up`, `down`, `right`, and `left`. A reward of +1 is received on reaching the goal, which ends the episode. Passing through the gray region between the start and hallway states produces a reward of  $-1$  per step, while all other transitions produce a reward of zero. While the two-room gridworld is deterministic, the four-room gridworld is stochastic: any chosen action causes the agent to move to the desired direction with probability  $2/3$ , with the agent instead moving in one of the other three directions with probability  $1/9$ . The discount factor is  $\gamma = 0.99$ .

#### A.2. Subtask specification

We define the reward-respecting subtasks such that the cumulant,  $C_t$ , is equal to the reward signal,  $R_t$ ; and  $\bar{w}^i = 1$  upon reaching the hallway state and  $\bar{w}^i = 0$  otherwise. We use an estimate of the value function for the equi-probable random policy as the value function in Eq. 4. We learn the estimate of the value function at the same time as we learn the option’s policy. We use TD(0) to learn the value of the equi-probable random policy, with a step-size  $\alpha = 0.9$  in the two-room gridworld and  $\alpha = 0.1$  in the four-room gridworld. We initialize  $\mathbf{w} = \vec{0}$ . We define shortest-path options such that  $C_t = 0$ ; and  $\bar{z}^i = 1$  upon reaching the hallway state and  $\bar{z}^i = 0$  otherwise.

#### A.3. Option learning for feature attainment

To learn the option’s policy, for both reward-respecting and reward-oblivious subtasks, we used *UpdateWeights&Traces* (UWT) to implement an actor-critic algorithm, as described in Eq. 6-8. We initialize the critic’s  $\mathbf{w}$  and  $\mathbf{e}$ , and the actor’s  $\omega$  and  $\mathbf{e}'$  parameters to be  $\vec{0}$ . We set  $\alpha = 0.1$  and  $\lambda = 0.0$  for the critic, and  $\alpha' = 0.1$  and  $\lambda' = 0.0$  for the actor. Finally,  $\beta$  is defined as in Eq. 9 for reward-respecting options and, for the reward-oblivious options, it is defined to be 1 upon reaching the hallway state or upon reaching the goal state, and to be 0 otherwise. In the two-room gridworld, we learn the options’ policies for 50,000 time steps, and in the four-room gridworld we learn the options’ policies for 200,000 time steps. We used a behavior policy that selected all four actions with equal probability:  $\mu(a|s) \doteq 0.25$  for all  $s \in \mathcal{S}$  and  $a \in \mathcal{A}$ . We executed this process 100 times in the two-room gridworld and 30 times in the four-room gridworld.

#### A.4. Model learning

We used the procedure outlined in Section 3 (Eq. 19-22) to learn the models for reward-respecting and reward-oblivious options, as well as the transition model for primitive actions only. As usual, we initialize all weights ( $\mathbf{w}_r^o$  and  $\mathbf{w}_{s'}^o$ ) and eligibility trace vectors ( $\mathbf{e}_r^o$  and  $\mathbf{e}_{s'}^o$ ) to be  $\vec{0}$ . We set the step-sizes  $\alpha_r$  and  $\alpha_p$ , to be 0.1 in the two-room gridworld and to be 0.05 in the four-room gridworld, and the eligibility trace parameters,  $\lambda_r$  and  $\lambda_p$ , to be zero. In the two-room gridworld, we learn the options’ models for 50,000 time steps, and in the four-room gridworld we learn the options’ policies for 200,000 time steps. We use the same number of time steps for both transition and reward models. We compute the RMSE reported in Figure 3 at each time step. We executed this process 100 times in the two-room gridworld and 30 times in the four-room gridworld.

#### A.5. Planning with options and approximations

We use approximate value iteration (AVI) as the planning algorithm in all experiments in the tabular case, following Eq. 24 and 25 closely. In that context, there are not many parameters to report. We perform 6,000 AVI updates in the two-room gridworld, and 20,000 AVI updates in the four-room gridworld. We consider value iteration has converged if a change smaller than  $10^{-4}$  is observed. As mentioned in the main text, we selected the states to be updated randomly. Finally, we executed this process 100 times in the two-room gridworld and 30 times in the four-room gridworld.

## B. Multiple options and stochasticity

In Section 6, we presented the outcome of the STOMP progression when multiple options were being used for planning. Due to space constraints, we only presented the planning performance of different options, briefly mentioning policy and model learning. In this section we present results in the four-room domain equivalent to those presented in Sections 2 and 3.

We use the four-room episodic gridworld depicted in Figure 8, with a start state in one room and a terminal goal state in another. Similar to the two-room gridworld, a reward of +1 is received on reaching the goal, which ends the episode. Passing through the gray region produces a reward of  $-1$  per step, while all other transitions produce a reward of zero. The discount factor is  $\gamma = 0.99$ . There are four actions, available in all nonterminal states: up, down, left, and right. Importantly, any chosen action causes the agent to *stochastically* move in the corresponding direction with probability  $2/3$  and in one of the other three directions with probability  $1/9$ . The parameters used were described in Appendix A. We now focus on discussing the results obtained at the end of each step of the option-learning and model-learning steps of the STOMP progression, which we did not discuss in the main paper.

### B.1. Option learning for feature attainment

As in Section 2, Figure 7 shows the convergence for the hallway-feature attaining subtasks, but now in the four-room gridworld. We used a behavior policy that selected all four actions with equal probability:  $\mu(a|s) \doteq 0.25, \forall s \in \mathcal{S}, a \in \mathcal{A}$ . The state-feature vectors were 1-hot, producing a tabular representation. The policy was of the softmax form with linear preferences:

$$\pi(a|s, \boldsymbol{\theta}) \doteq \frac{e^{\boldsymbol{\theta}^\top \boldsymbol{\phi}(s,a)}}{\sum_b e^{\boldsymbol{\theta}^\top \boldsymbol{\phi}(s,b)}}, \quad (26)$$

where the state-action feature vectors  $\boldsymbol{\phi}(s, a) \in \mathbb{R}^{d'}$ ,  $\forall s \in \mathcal{S}, a \in \mathcal{A}$  were again 1-hot or tabular. We ran for 200,000 steps and averaged the results over 30 runs.

Figure 7 depicts the root mean squared error, throughout time, between the estimated subtask value,  $\hat{v}(S_t, \mathbf{w}_t^h)$ , for the subtask for attaining the  $h$ th feature, corresponding to one of hallway states, and the *optimal subtask value*,  $v_*^h(s) \doteq \max_{\pi, \beta} v_{\pi, \beta}^h(s)$ , for all  $s \in \mathcal{S}$ . The plots are organized in clockwise order for hallways H1, H2, H3, and H4. These curves show actor-critic is able to effectively learn the correct option policy. The main difference from the plot in Figure 2 is the duration of learning. This is because the environment is bigger and it is stochastic, requiring more samples for accurate value estimation. For the hallway-H4-reaching subtask, we see more samples would be beneficial for a more accurate option, but this does not seem to impact the planning performance shown in Figure 4.

Figure 8 depicts the corresponding learned option policies. As before, the option terminates either at the bottleneck state or at the goal state, as shown in red. Reward-respecting options trade-off rewards, the value of the state, and the stopping bonus. Reward-respecting options do take into consideration the fact that the environment’s stochasticity is not under the agent’s control. For the most part, the options take the shortest path to the appropriate hallway or the goal state, but the

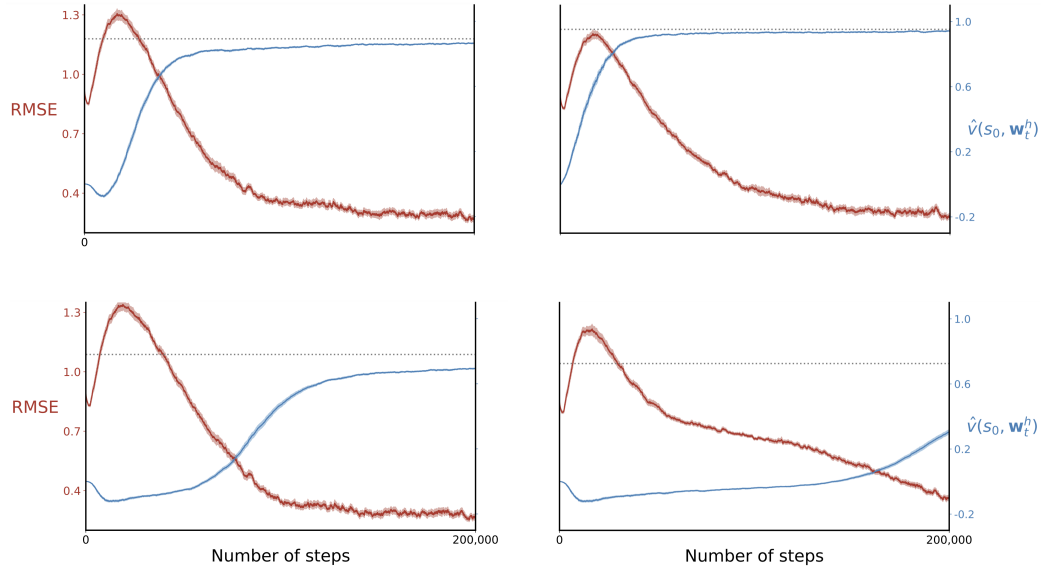


Figure 7. The off-policy learning algorithm applied to find the optimal option for the reward-respecting subtask for attaining the hallway features (H1, H2, H3, and H4, clockwise). The data comes from a policy in which all four actions are selected with equal probability. The plot shows the progress of learning. The blue line (right scale) shows the value of the start state for the learned option, and the red line (left scale) shows the RMSE between the learned and optimal value functions. Each line is averaged over 30 runs and the shading represents the standard error.

uncontrolled stochasticity and the negative reward region causes some options to take a longer path. For example, when in the SW room, options sometimes take the roundabout way to reach H3 and H4.

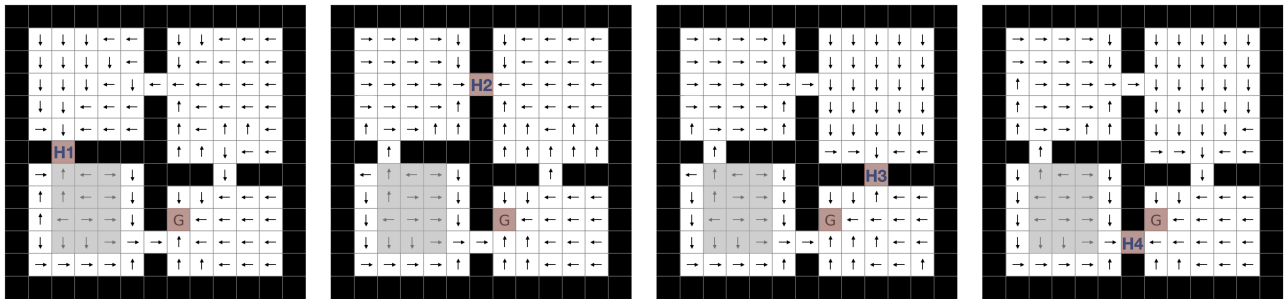


Figure 8. Illustration of reward-respecting options learned in a stochastic gridworld. Passing through the gray region between the start and hallway states produces a reward of  $-1$  per step, while all other transitions produce a reward of zero. Reaching the goal state produces a reward of  $+1$ . Stochastic transitions make states close to the shaded region less desirable due to the natural uncertainty over their return.

## B.2. Model learning

We used the UWT procedure we described in the main paper to learn the models in the four-room gridworld. As shown in Figure 9, this procedure allows us to efficiently learn both transition and reward models. The plots are organized in clockwise order for hallways H1, H2, H3, and H4. The main difference from the plot in Figure 3 is the duration of learning. This is because the environment is bigger and it is stochastic, requiring more samples for accurate value estimation.

We also evaluated the impact of planning with imperfect models, using approximate value iteration, as described in the main paper. The final performance is what we report in Figure 5b. Here we report the performance of planning not when the model was learned for 200,000 time steps, but when it was learned for 10k, 20k, 30k, and 40k time steps. Planning leads to near-optimal performance using an imperfect model trained for 50,000 steps. Further training improves model error but does not significantly improve planning in this environment.

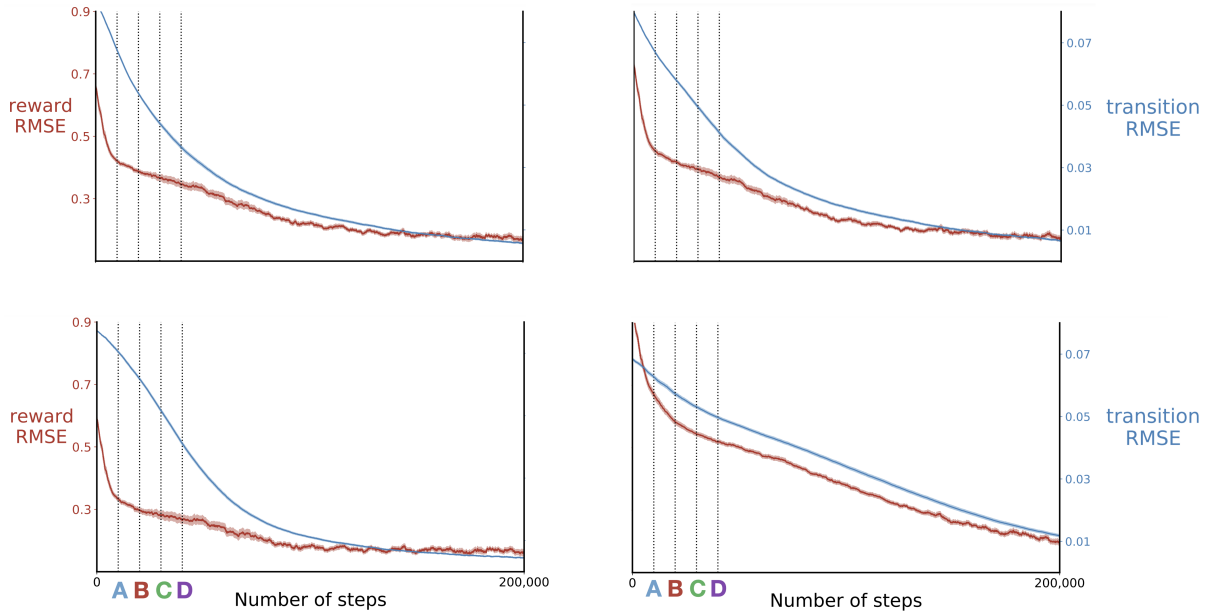


Figure 9. Transition and reward models are efficiently learned online (H1, H2, H3, and H4, clockwise). The red line (left scale) shows the root mean square error (RMSE) between the learn reward model for the option and the idealized reward model. The blue line (right scale) shows the RMSE between the learned transition model for the option and the idealized state-transition model. The state-transition model captures discounting and termination. All lines were averaged over 30 runs and the shading represents the standard error.

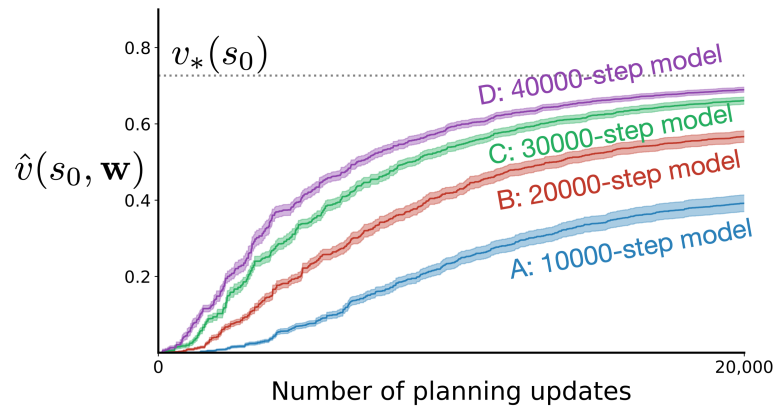


Figure 10. Performance of planning for learned, approximate models with different levels of accuracy. In this environment, 50,000 steps of model learning is sufficient to achieve near-optimal planning performance. All lines were averaged over 30 runs and the shading represents the standard error.